NASA Contractor Report 198311

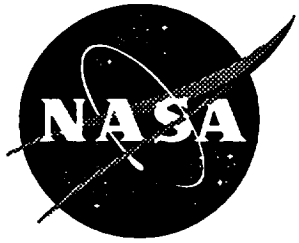

Results of Tests Performed on the Acoustic Quiet Flow Facility Three-Dimensional Model Tunnel

Progress Report on the D.S.M.A. Design

P. S. Barna
Lockheed Engineering & Sciences Company
Hampton, Virginia

Contract NAS1-19000

April 1995

National Aeronautics and
Space Administration
Langley Research Center
Hampton, Virginia 23681-0001

RESULTS OF TESTS PERFORMED ON THE ACOUSTIC QUIET FLOW FACILITY THREE-DIMENSIONAL MODEL TUNNEL PROGRESS REPORT ON THE D.S.M.A. DESIGN

by
P.S.BARNA

SUMMARY

The test results briefly described in this report were obtained on the three-dimensional 1:48 scale tunnel modeled on the design proposed by Messrs. D.S.M.A. Corporation. More particularly, while the test chamber dimensions were indeed scaled down in the ratio of 1:48, including the contraction and the collector as well, the duct system itself leading to and from the chamber was adapted to suit laboratory conditions and space limitations.

Earlier tests with the two-dimensional model showed that blowing mode was preferred as against the suction mode, hence all tests were performed with blowing only. At the exit of the contraction the maximum airspeed attained with the 1 HP blower unit was about 200 ft/sec. This airspeed may be increased in future if desired.

The test results show that pressure recovery in the diffuser was about 34 percent due to the large blockage at its entrance. Velocity traverses taken across the diffuser entrance explain the reason for this blockage. Recirculation, studied with both, hot-wire anemometry and flow-visualization techniques, was largely affected by the design of the test chamber itself and the amount of vent-air admitted to the chamber. Vent-air helped to decrease the level of turbulence.

DESCRIPTION OF THE TEST MODEL

The three-dimensional test model is the replica of the full-scale design as shown in figure 1, which was submitted by Messrs. D.S.M.A. Corporation in 1992. The test model was scaled down in a ratio of 1:48, and the essential features of the test chamber are shown in figure 2. It is noted, that prior to building the 3-D model, tests were performed on a 2 dimensional model of the same scale. Results of tests performed on the 2-D model were presented in a report issued in 1994 (ref 1).

The test chamber surrounding the test section, the diffuser, and the circular "chimney", was fabricated using transparent plexi-glass, while the ducting from the air supply was formed from sheet metal. The exit of the "chimney" was provided with a throttling device to adjust airflow. The contraction was made of fiberglass. Upstream of the contraction a honeycomb was inserted immediately followed by a double screen, one with a coarse and another with a fine mesh. Also, the air vent was provided with a fine mesh screen.

A view of the complete scale model tunnel is shown in figure 3 where the air supply unit (a centrifugal fan) is visible in the foreground, while the vertical exit chimney occupies the background. A view of the test chamber is shown in figure 4 with its vent-air intake at the top and with the contraction and diffuser intake inside the enclosure.

INSTRUMENTATION

A variety of instruments were employed in the testing. Pressures were obtained with an electronic " Mensor" gage and both horizontal and vertical velocity traverses were established with pitot tubes, pitot cylinders and hot wires. Flow rates were measured with orifice plates either having a 3.5 or a 4 inch circular opening. The orifice plates were located in the chimney, about 12 inches from its exit and the flow rates were carefully monitored.

In order to study the recirculating flow taking place outside the main jet issuing from the contraction, a flow visualization technique was introduced using helium filled soap bubbles which moved with the air at the same speed. High speed movie cameras recorded the motion.

The hot wires were employed for both: measuring the turbulence level and for measuring air velocity. Accordingly, an r.m.s. meter was used for turbulence measurements while an "IFA" voltmeter was establishing air speed. An oscilloscope was showing visual changes in the turbulence levels.

METHOD OF TESTING

Calibrations

Hot wire calibrations were performed in three stages. In the first stage a low velocity air stream was set up using a large area inlet duct to a variable speed fan and a small area outlet area where the air velocity could be satisfactorily established. The area ratio between inlet and outlet was 8:1. In this set-up, shown in figure 5, speed could be varied from about 2 ft/sec to about 20-25 ft/sec. In the second stage another set up was used, which consisted of a first divergent then convergent circular duct, ending in a parallel section of about 0.5 inches diameter, as shown in figure 6. By varying the fan speed this set-up allowed the calibration to reach about 100-110 ft/sec. when using the same fan as before for the low speed calibration. In the third stage the probe was placed inside the model tunnel and the calibration extended to about 180-200 ft/sec. The procedure was repeated to cover three hot wire probes employed.

To establish the flow rates various calibrations were employed. It was first assumed that the orifice could be used for the total flow rate, being a sum of the flow through the contraction and through the air vents. To calibrate the contraction the air vent was blocked so that the flow through the contraction equaled the flow through the orifice. In both, the orifice meter and the contraction, static ports were employed to find the flow rates. Finally, the flow at exit of the contraction was traversed in both direction with the hot wire

probe. This procedure checked the orifice and the contraction flow.

Experience shows that when a wire breaks, the replacement wire needs a fresh calibration. Sample calibrations are shown in figure 7, where air velocity, U ft/sec is plotted against electric output E volt, measured with the IFA meter.

Pressures

Static pressures were measured at relevant points, and their locations are shown in figure 8. In particular, port 1 was located at the exit duct of the fan , 2 upstream, 3 downstream from the honeycomb and screens, 4 at contraction entry and 5 at contraction exit. At 5, the static port was provided with the static side of a pitot tube. Port 6 measured the ambient pressure inside the enclosure, while port 7,8 and 9 were located at diffuser entry and exit, respectively. Finally, ports 11 and 12 were located up- and downstream from the orifice plate.

Total pressures were measured with small pitot tubes of 0.016 in. diameter fastened to 0.125 ins. diameter tubes exending right across the test chamber which could be manipulated from outside by using specially designed mechanisms for both horizonal and vertical traverses.

TEST PROCEDURES

Testing always began with establishing the pressure distribution along the circuit. Generally three sets of distributions were taken: one with the air vent fully blocked, one with free entry (blockage completely removed) and one with screen stretched across the air-vent opening. The screen used was a 100 mesh fine copper screen with fairly high resistance, noted as the "D" screen in the tests.

Pressure distribution test were followed by measurements of the velocity, first across the exit from the contraction and second, across the inlet to the diffuser.

Hotwire tests were limited to traverses across the entire stream

right upstream from the diffuser entry (noted as location 7).

TEST RESULTS

Pressure distribution

Figure 9 shows the variation of static pressure along the circuit under condition when no ventilating air was allowed to enter the test chamber (air vent blanked off). When following the line, one finds a small drop in pressure between locations 1 and 2. This change, about 0.75 p.s.f. is mostly due to acceleration, while the larger drop, between 2 and 3, is due to the marked resistance of the honeycomb and the screens. The massive drop between 4 and 5 is due to the increase in speed due to the contraction of an area ratio of about 20 to 3, resulting in a predictable change of about 51.5 p.s.f. This causes sub-atmospheric pressure of about -11 p.s.f. at contraction exit.

The rise in pressure between 5 and 6 does not represent a physical recovery process, because port 6 is measuring the pressure in a corner of the chamber. However the rise between 7 and 9 is significant because it represents diffuser recovery. A further, albeit small diffusion takes place between 9 and 11. The drop in pressure between 11 and 12 is used for establishing the total flow rate through the orifice, while the drop between 12 and exit leads to atmospheric pressure. (Please note that port 8 was not participating).

With the air-vent open the static pressure distribution changes to some extent, as shown in figure 10. While the total flow rate remains about the same, the flow through the contraction becomes smaller owing to the "ejector" effect the jet produces. And while the pressure at the beginning and at the end of the circuit appears the same, 56 p.s.f. at location 1 and atmospheric at exit, the pressure at 5 is above atmospheric, and remains so all the way to exit.

The tests just described were obained with either the blocked or the open air vent provided with a screen having 100 mesh to the inch, called the D screen. The orifice employed had a 3.5 ins. diameter and the height h of the throttle was 1.8 ins.

Flow distribution

a) Velocity traverses obtained at exit from the contraction (location 5) show substantially uniform distribution for both, blocked and air-vented conditions. Figures 11 and 12 show the horizontal, while 13 and 14 show the vertical distribution. Small deviations from uniformity may be detected and are considered effects due to the resistance created by the stems of pitot heads (or hot wires) supported by the long stem. Small build-ups of the boundary layer are also noticeable at each end of the traverses and these are considered normal. The traverses indicate that almost 100 percent of the flow is uniform, hence the design of the contraction is satisfactory.

b) Altogether different distributions were observed at inlet to the diffuser, as shown in figures 15, 16 and 17. In figure 15, showing horizontal distribution in the centerplane of the air intake, only 59 percent of the flow is uniform and may be seen roughly symmetrical about the center line. However, outside this "central " portion flow velocity rapidly decreases to zero. It is of considerable interest to observe that zero velocity is not experienced at the wall but at some distance inboard on both sides. Figures 16 and 17 show vertical traverses at air intake with blocked and free ventilation. With blocked air vent, the uniform portion is only about 51.5 percent of the traverse distance, while it was found somewhat better with ventilation. These are the results of the air intake being too wide and too high.

The "missing" portion of the flow near the wall represents reverse motion. This may be visually observed by placing a tuft near the walls at the air intake. One finds the tuft being rejected, turned around and moved out from the diffuser's intake by the reverse flow.

Diffuser performance

The "DIFFUSER DATA BOOK" (ref. 2) defines recovery as the pressure rise along the diffuser related to the dynamic pressure prevailing at the center of the intake. Thus

$$R = (P9 - P7) / 0.5 \rho V^2$$

where o is the density of air.

Diffuser recovery with the DSMA diffuser design was found about the same with the D screen as with the blank, namely

$$R = 0.34$$

When compared with a similar design shown in the DATA BOOK under Flat Diffusers, this figure appears rather low. In the DATA BOOK one finds about 0.58 for recovery, for a blockage of 8 percent. (Under similar design the area ratio AR and the length-to-width ratio L/w is the same). Apparently blockage in the DSMA design is much higher probably due to the reverse flow at the diffuser entry and possibly other effects. (See Appendix I).

Turbulence

Turbulence was measured with hot-wire using the r.m.s. meter coupled with the IFA voltmeter. Data were obtained for the horizontal and vertical centerlines about 0.25 ins. upstream from diffuser entry, and the results are shown in figures 18, 19 and 20.

Figure 18 shows the horizontal traverse with the air-vent open and using the D screen. The traverse extended across and close to the full width of the test chamber (14.5 ins.), the jet centerline being located about 62 percent of the width. The wide area of the chamber appears on the left and the narrow part on the right from the jet center. It appears that air velocity rises sharply from a few ft/sec to about 190 ft/sec at the plateau where its width is about 10 percent of the total, that is about 1.45 ins. Outside the main jet, the recirculating flow velocities may be estimated as being between 2 and 3 ft/sec. Turbulence u* (see Appendix II) has two maximas and three minimas, the lowest minima value observed in the jet center was about 0.02. It is of interest to note how the turbulence level increases in the shear layer created inside the main jet's boundaries. Similarly, some rise in turbulence may also be noticed near the solid walls, where u* "kicks up" owing to the presence of the boundary layer. Also of interest is to note that the turbulence peaks have unequal values: 0.65 at x/w=0.53 and 0.38 at x/w=0.725. The rise and fall in the vicinity of these peaks seems

rather steep.

Figure 19 shows the vertical traverse at the same location with the air vent open when using the D screen. It appears at once that the distributions of u* is more symmetrical owing the the jet center being at half the distance between floor and ceiling. The jet plateau seems again 10 percent of the traverse distance, this time 1.05 ins. wide. The turbulence peaks appear about the same u* = 0.61 and 0.625 respectively, while the minima is about 0.02 again near center.

With the air vent blocked, distribution of turbulence markedly changes, as shown in the horizontal traverse presented in figure 20. On the wide side of the chamber some humps and hollows follow the peak. The hump, located at x/w = 0.35, peaks at u* = 0.39 , a marked increase from 0.14 shown on figure 18. The increase in turbulence with blocked air vent also showed up later in visual studies.

Studies with flow visualization

The simplest test at diffuser entrance was performed with a tuft attached to a thin rod that could be entered into the chamber through a small opening. The tuft was part of a graduation tassle, made of nylon and thus very inert. Manipulating the rod to let the tuft enter the diffuser, one may traverse across the flow and observe the tuft stretched out by the high velocity until the side wall of the diffuser is approached. All of a sudden the tuft reverses its direction and is blown out of the diffuser. This clearly demonstrates reverse flow at the diffuser entrance.

Flow visualization was also performed with helium filled tiny "soap" bubbles. This procedure was employed to visually observe the recirculation in the spaces between the main jet and the walls of the test chamber. The bubbles were generated outside the chamber and were introduced into the chamber through a 5/16 in. diameter pipe. The bubbles were small, about 1/8 of an inch in diameter and were generated at a rate of about 200 per second. High speed film cameras, operated by NASA photographers recorded the movement of the bubbles which moved around on various quasy circular clockwise paths.

DISCUSSION OF THE RESULTS

Results of the tests show that the DSMA design of the Acoustic Quiet Flow Facility may have to be improved mainly because of the low efficiency of recovery of the diffuser. Methods for improving efficiency demand that the blockage at diffuser entrance to be low, preferably below 10 percent. Even if the geometry of the diffuser is correct, in some instances it is rather difficult to obtain the desired blockage owing to the adverse history of the flow, which is the case of a jet entering a diffuser. Experience shows the changes associated with a jet issuing from a nozzle. Even if the jet leaving the nozzle shows a perfectly uniform flow distribution , marked changes downstream from the nozzle exit may be anticipated (Ref.3).

The tests show the shape of the flow distribution at the diffuser inlet with the uniform part being only a fraction of the intake of the diffuser. The reverse flow observed during the tests is held responsible for the large blockage that causes the inefficient recovery.

Efficient recovery in the diffuser is especially important when considering blowing mode operation. Assuming near atmospheric pressure in the test chamber and knowing that atmospheric pressure also prevails at the exit of the exhaust system, it remains for the conversion of kinetic energy of the jet to adequately provide for the diffuser and other frictional losses encountered in the exhaust system. Thus the efficient conversion of kinetic energy into pressure is vitally important.

It may be possible to improve the recovery of the diffuser by installing a suitable collector upstream of the diffuser intake and also provide a suitable gap between collector exit and diffuser inlet. The tests performed earlier on the two-dimensional model may provide guidance (Ref. 1) although it may be conceivable that the 3-D model is more complex and therefore more difficult to handle than the 2-D model. The tests showed no undesirable effects of the air vent being placed on top of the chamber.

REFERENCES

1. Barna, P. S.: Results of Tests Performed on the Acoustic Quiet Flow Facility Modified Two-Dimensional Model Tunnel. Final Report, Phase 1, Lockheed Engineering & Sciences Company, January 1994.

2. Runstadler, P. W., et al.: Diffuser Data Book. CREARE Inc., TN 186, May 1975.

3. Abramovich, G. N.: The Theory of Turbulent Jets. M.I.T. Press, 1963.

APPENDIX I

The DIFFUSER DATA BOOK defines efficiency of recovery R as the pressure rise divided by the dynamic head at the center of diffuser entry. With the symbols used in the tests of the DSMA diffuser

$$R = (P9 - P7)/ 0.5 \rho Vc^2$$

A typical set of data gives P9 = 17.3 psf, P7 = 3.6 psf and Vc = 186.5 ft/sec.

With $0.5 \rho = 0.00116$, one obtains upon substitution into the above equation

$$R = 0.34 = 34\%$$

Diffuser recovery was found about the same with vented or blanked off flow.

APPENDIX II

Turbulence was first measured with the r.m.s. meter and a value of u' was obtained. The IFA voltmeter produced the air speed U and the data were fed into the computer in order to obtain a fifth degree polynomial fit equation U = f (E). To obtain dU/dE the equation was differentiated and plotted against E. Finally, the turbulence level u'/U was multiplied with dU/dE, giving

$$u^* = u'/U \ (dU/dE)$$

(Note: both U and dU/dE were plotted against E measured by the voltmeter).

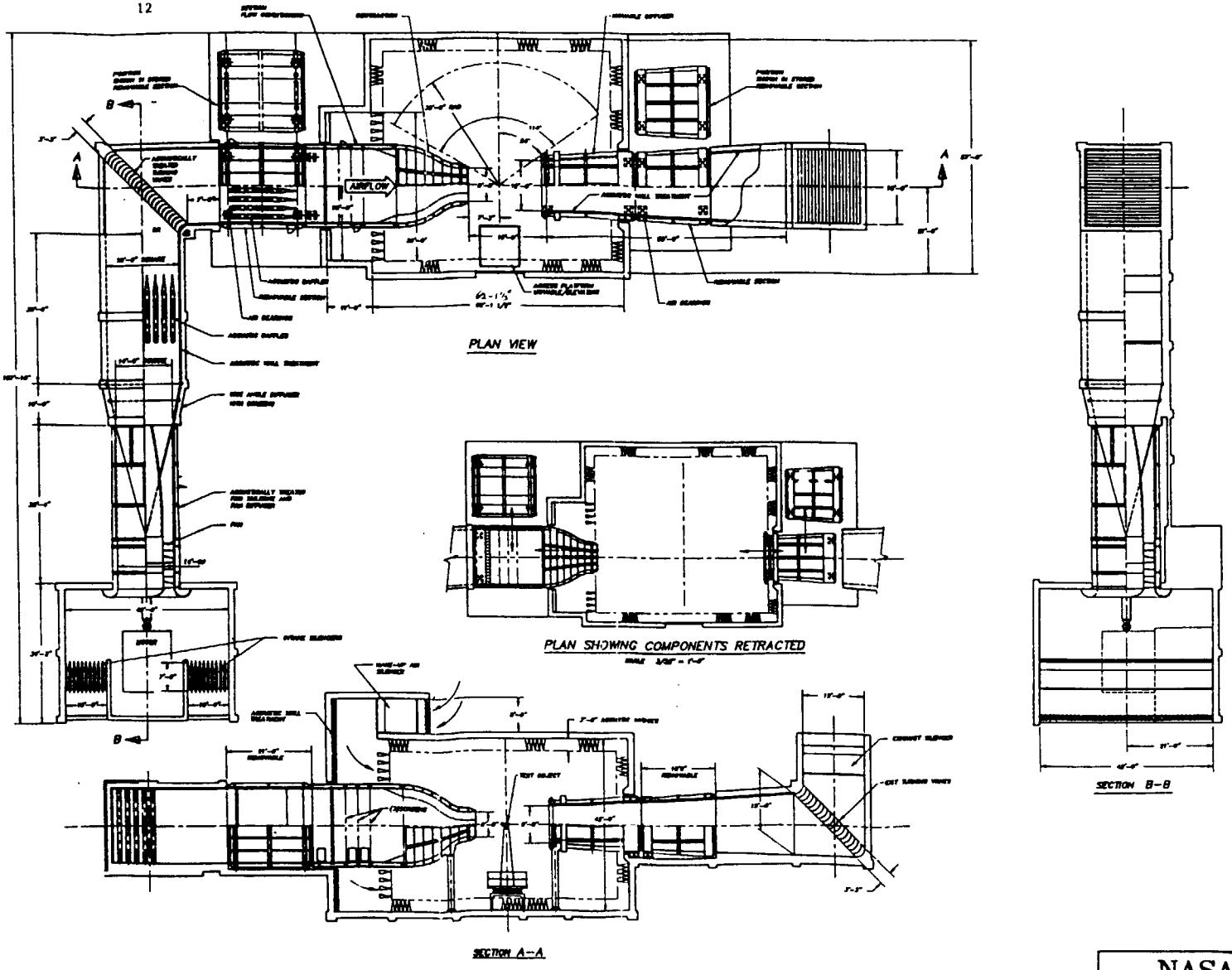

FIGURE 1. FULL SCLE PLAN OF THE A.Q.F.F. TUNNEL BY D.S.M.A.

GENERAL ARRANGEMENT

NASA
QUIET FLOW FACILITY
OFF E DWG-001

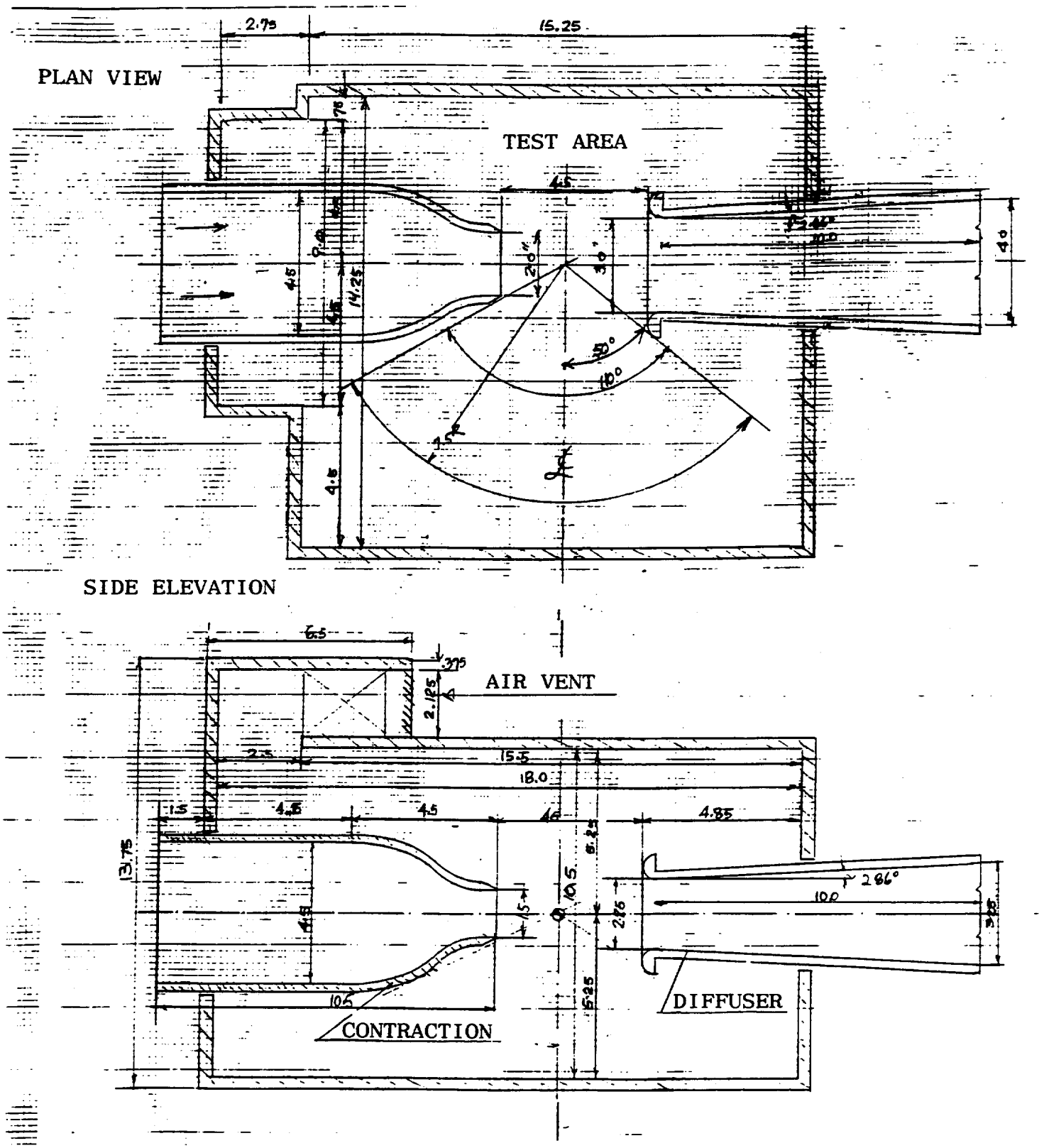

FIGURE 2. SCALE MODEL OF THE D.S.M.A. TESTING CHAMBER

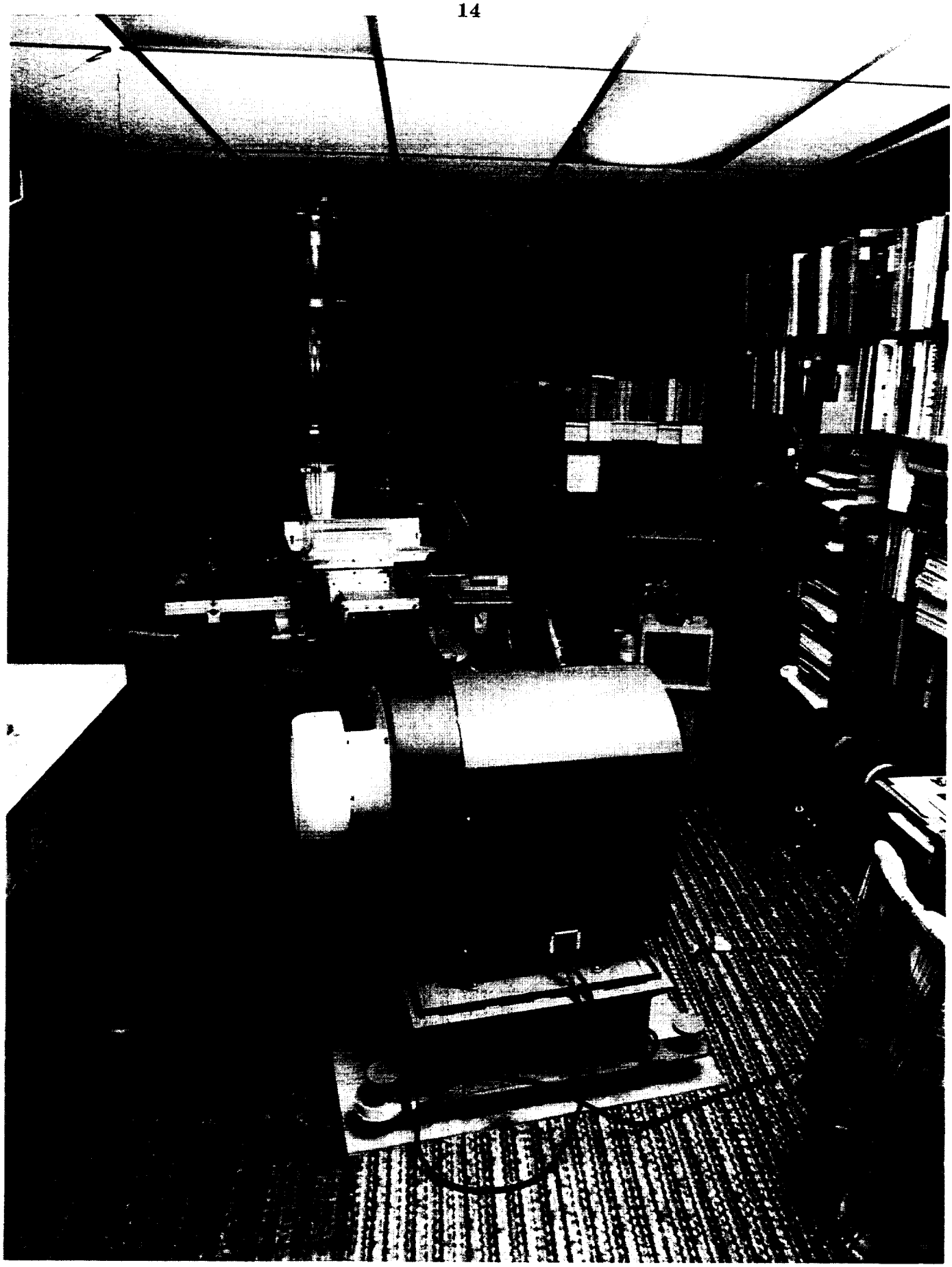

FIGURE 3. VIEW OF THE COMPLETE SCALE MODEL TUNNEL

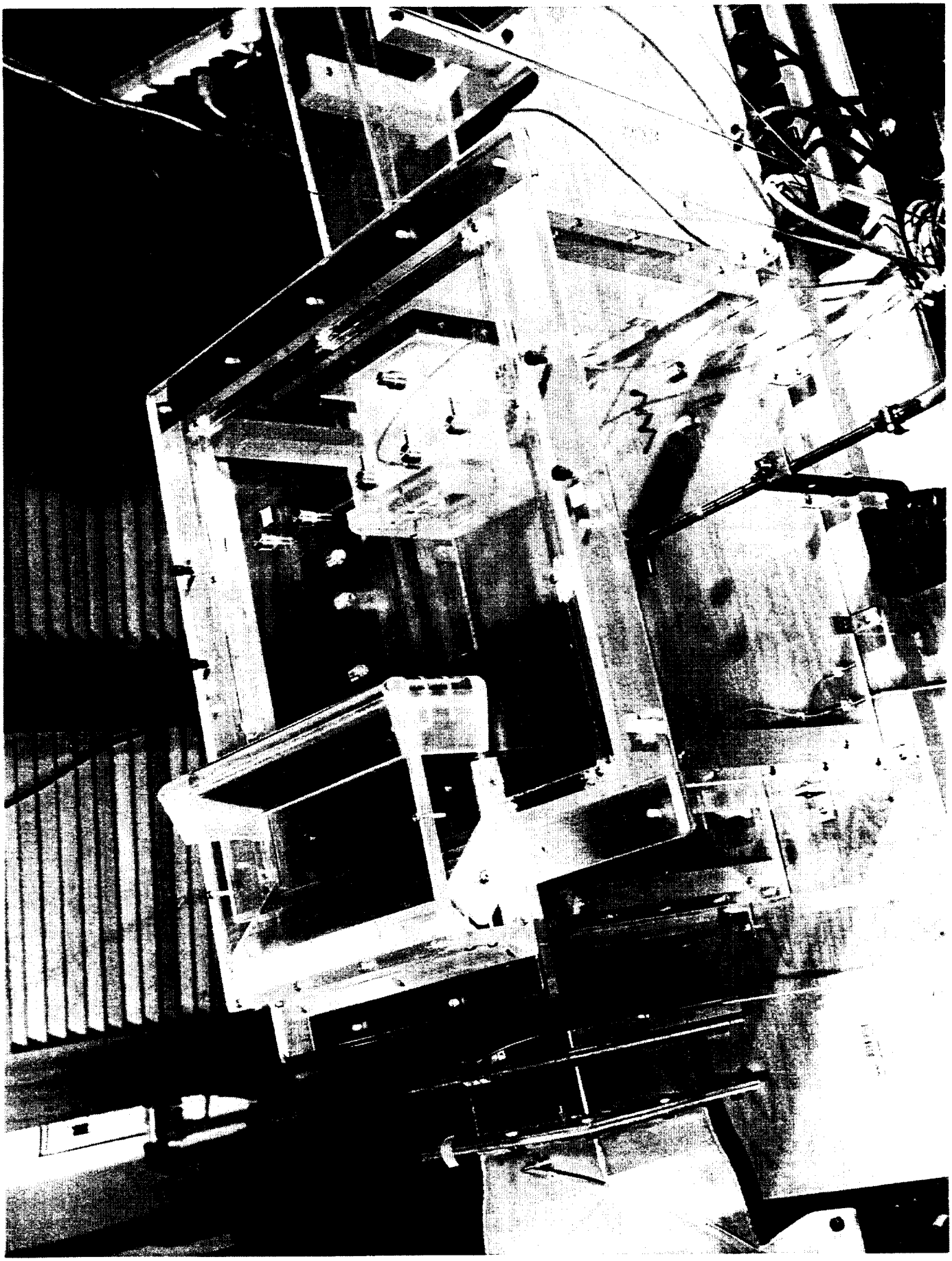

FIGURE 4. VIEW OF THE D.S.M.A. SCALE TEST CHAMBER

FIGURE 5. HOT-WIRE CALIBRATION SET-UP FOR LOW SPEED

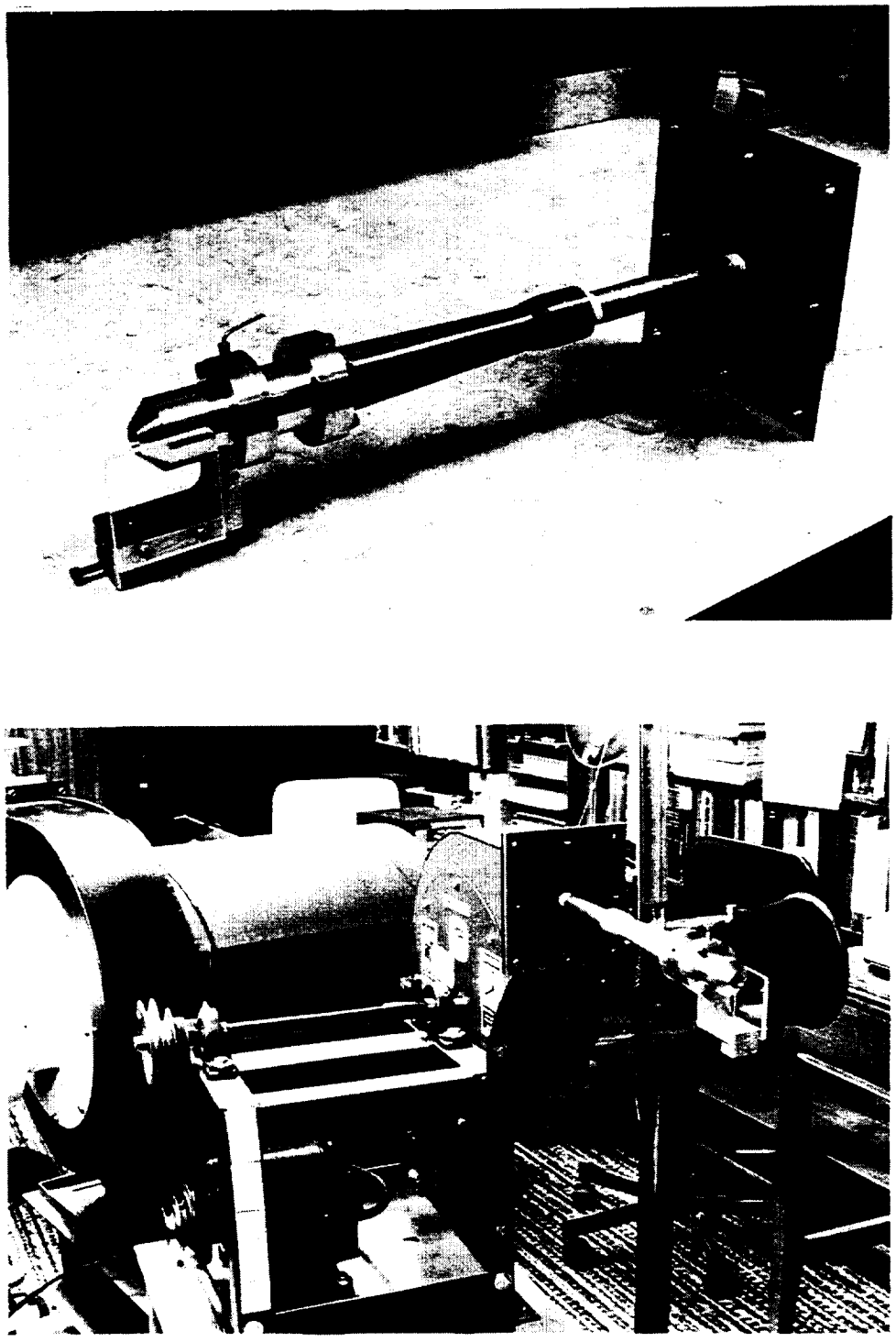

FIGURE 6. HOT-WIRE CALIBRATION SET-UP FOR HIGH SPEEDS

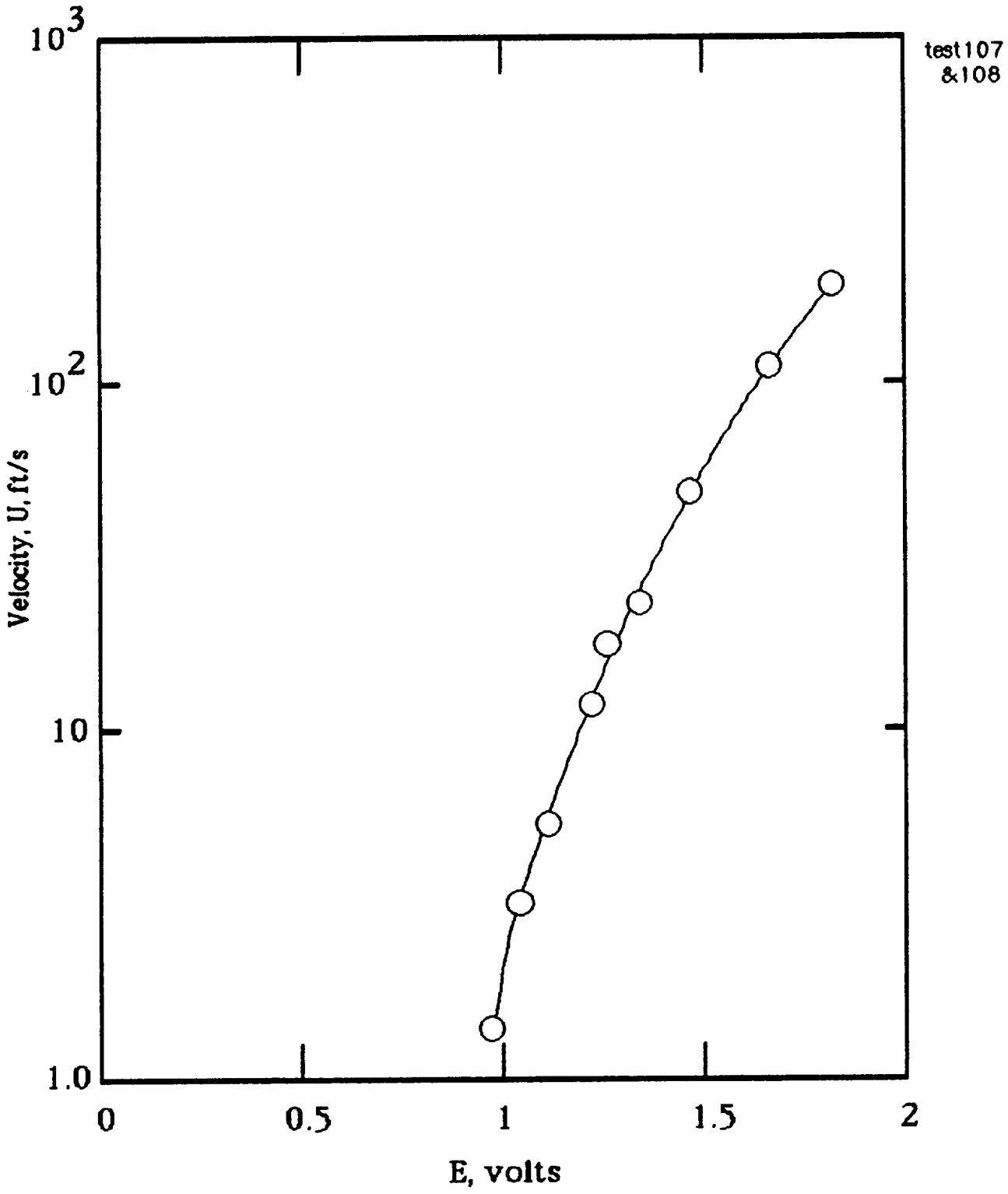

Figure 7. Calibration sample of the #2 hot-wire.

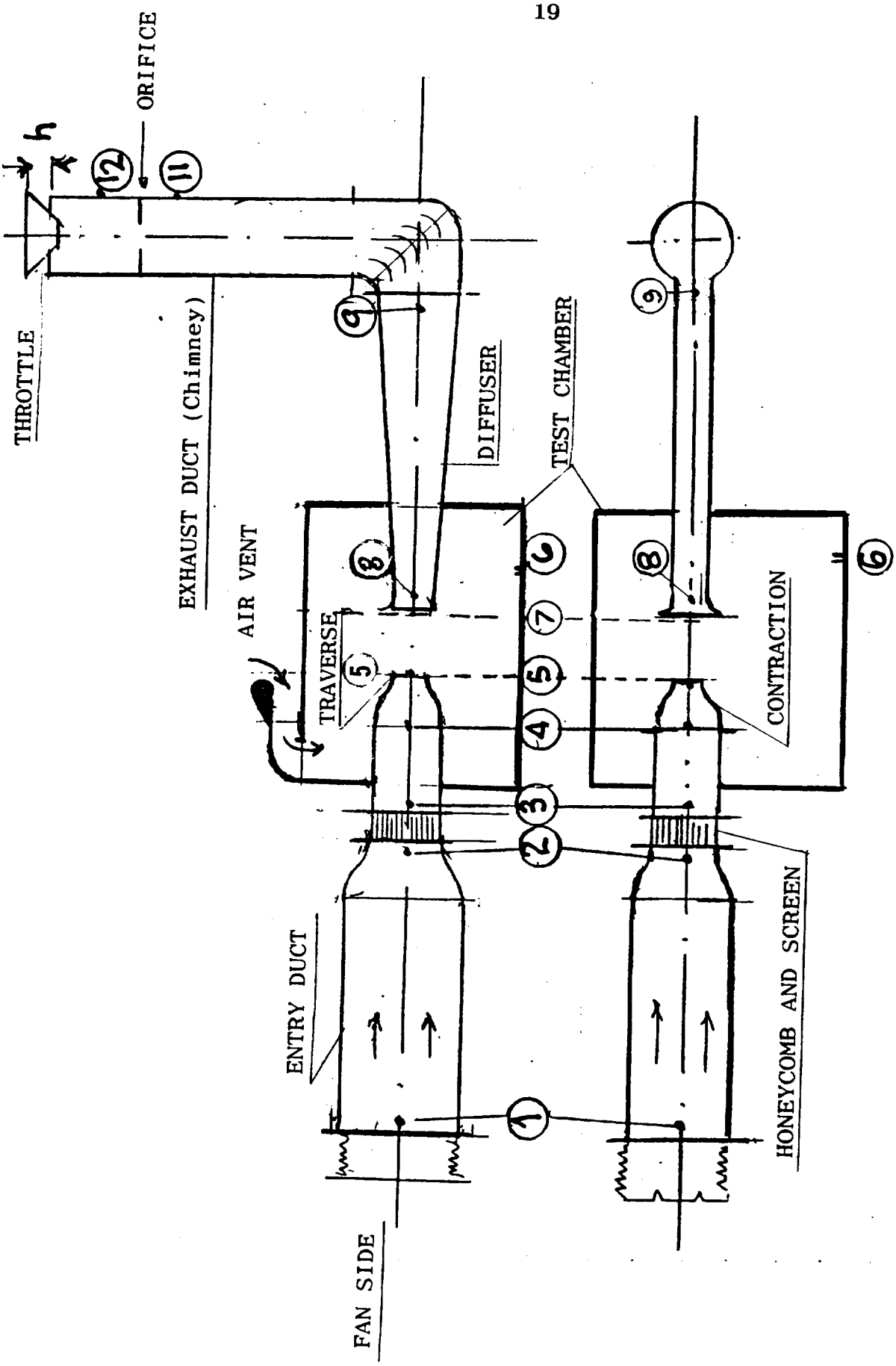

FIGURE 8. DISTRIBUTION OF STATIC PORTS ALONG THE TUNNEL CIRCUIT

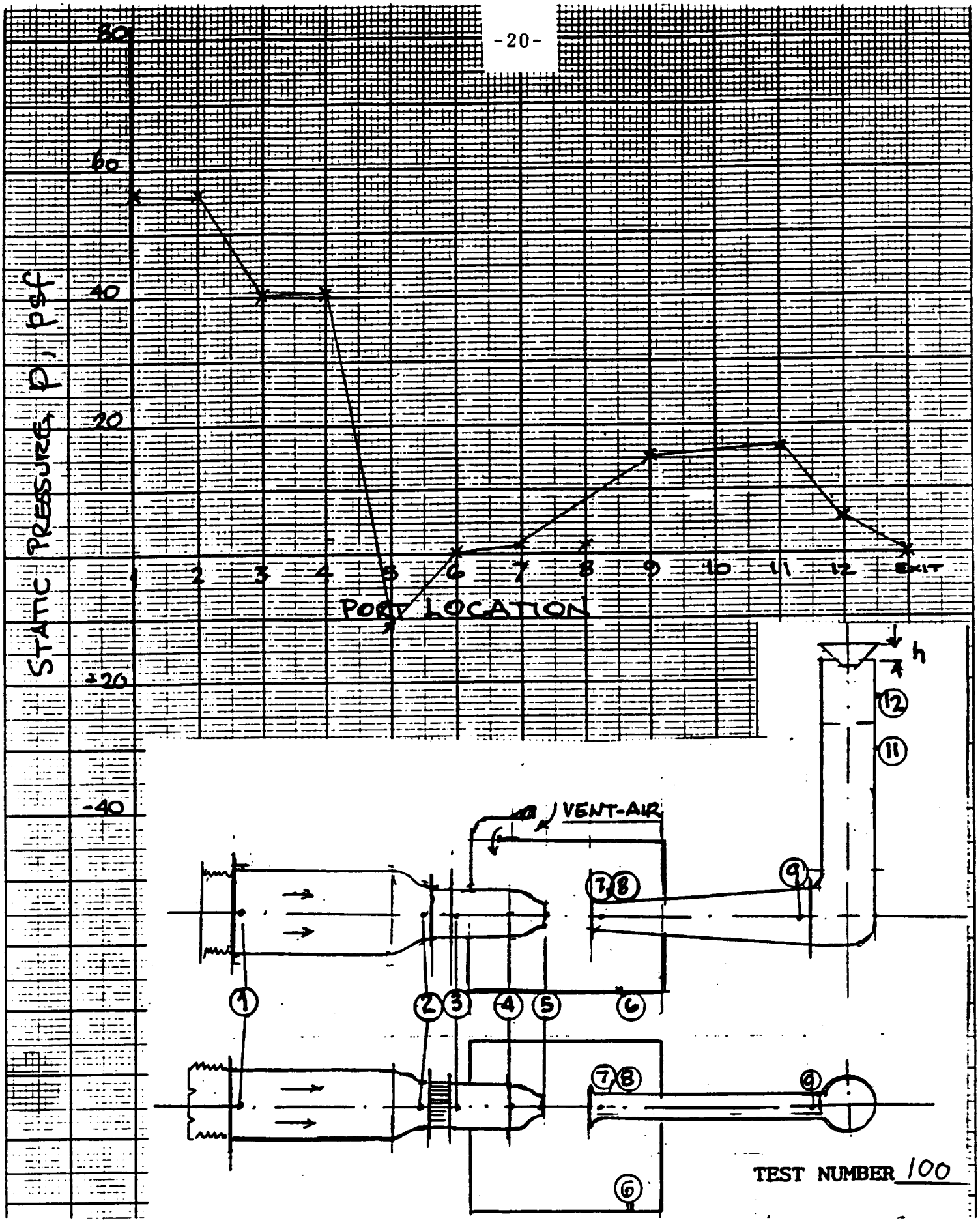

FIGURE 9. VARIATION OF STATIC PRESSURE ALONG THE DSMA CIRCUIT WITH THE AIR VENT BLOCKED OFF

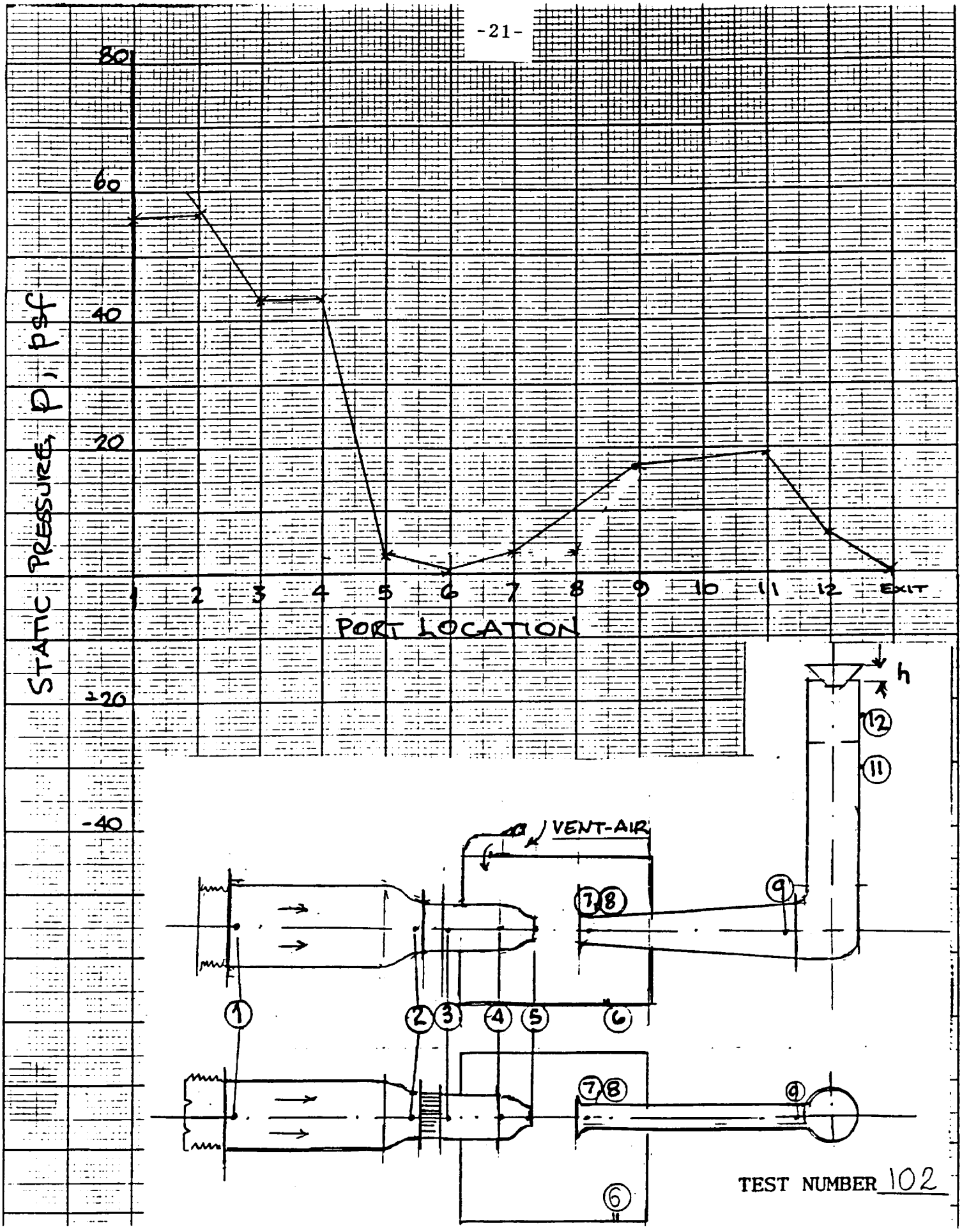

FIGURE 10. VARIATION OF STATIC PRESSURE ALONG THE DSMA CIRCUIT WITH THE AIR VENT OPEN USING D SCREEN

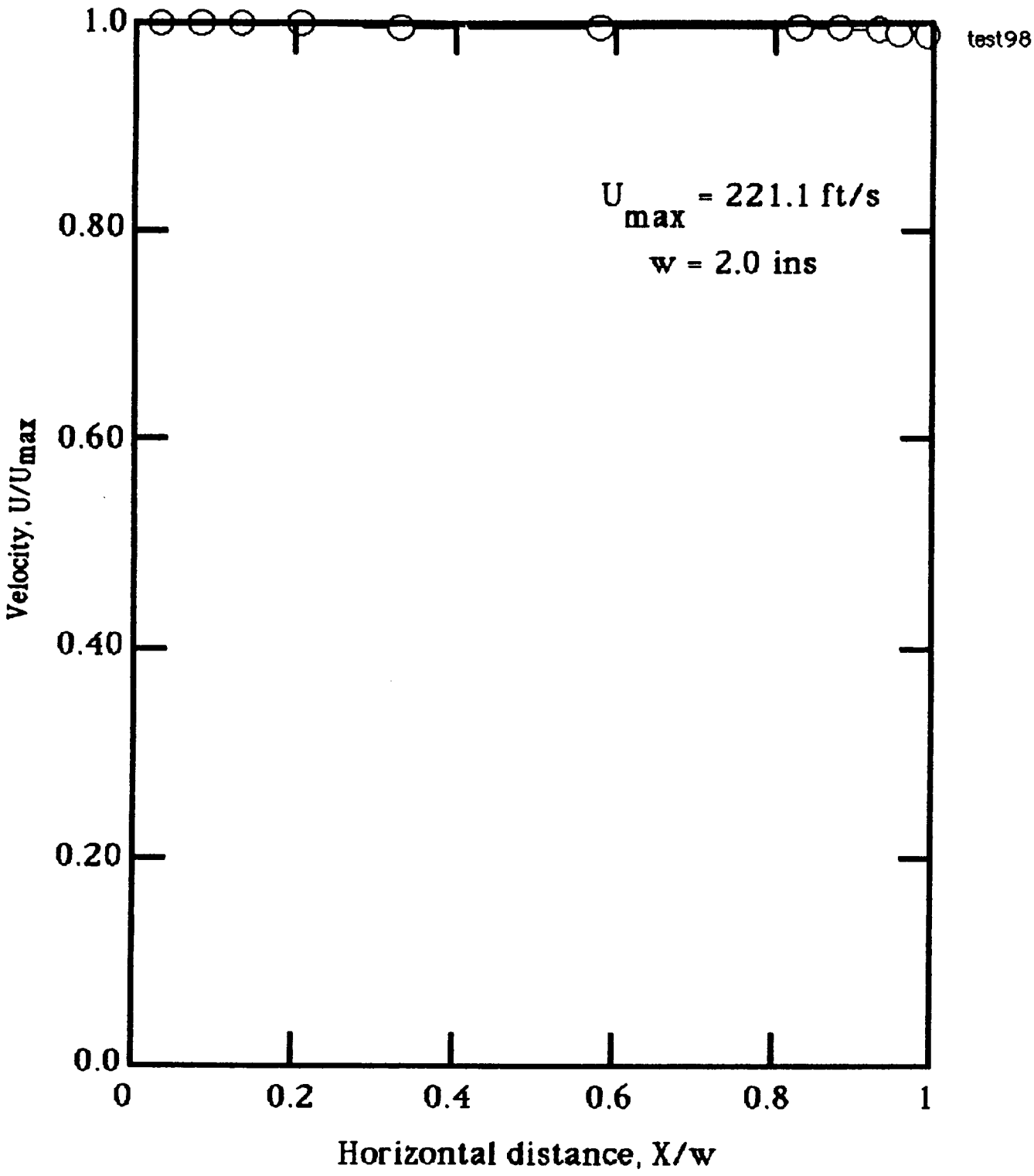

Figure 11. Horizontal variation of flow velocity across the centerline of the contraction exit plane with the air vent closed.

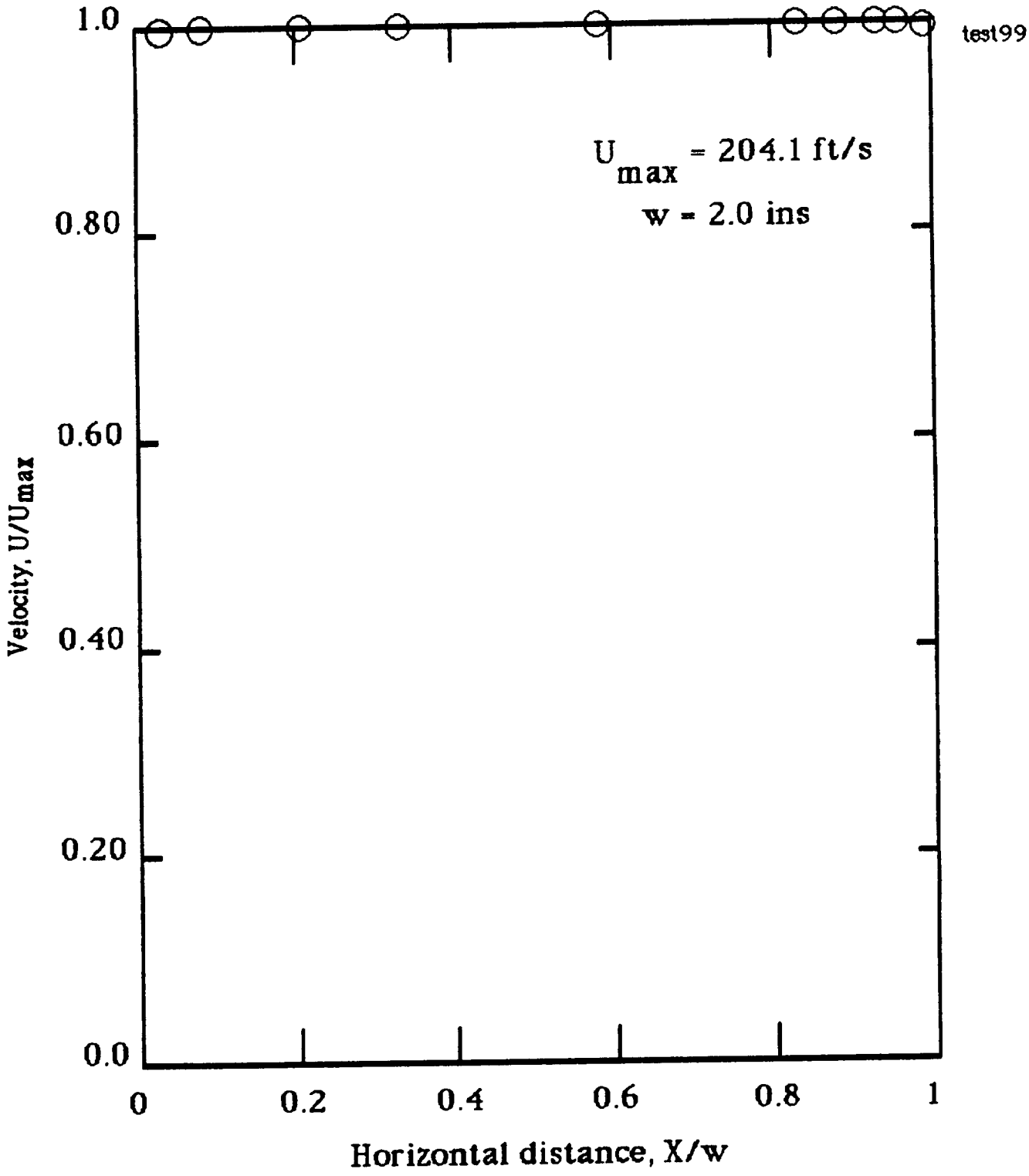

Figure 12 Horizontal variation of flow velocity across the centerline of the contraction exit plane with the air vent open.

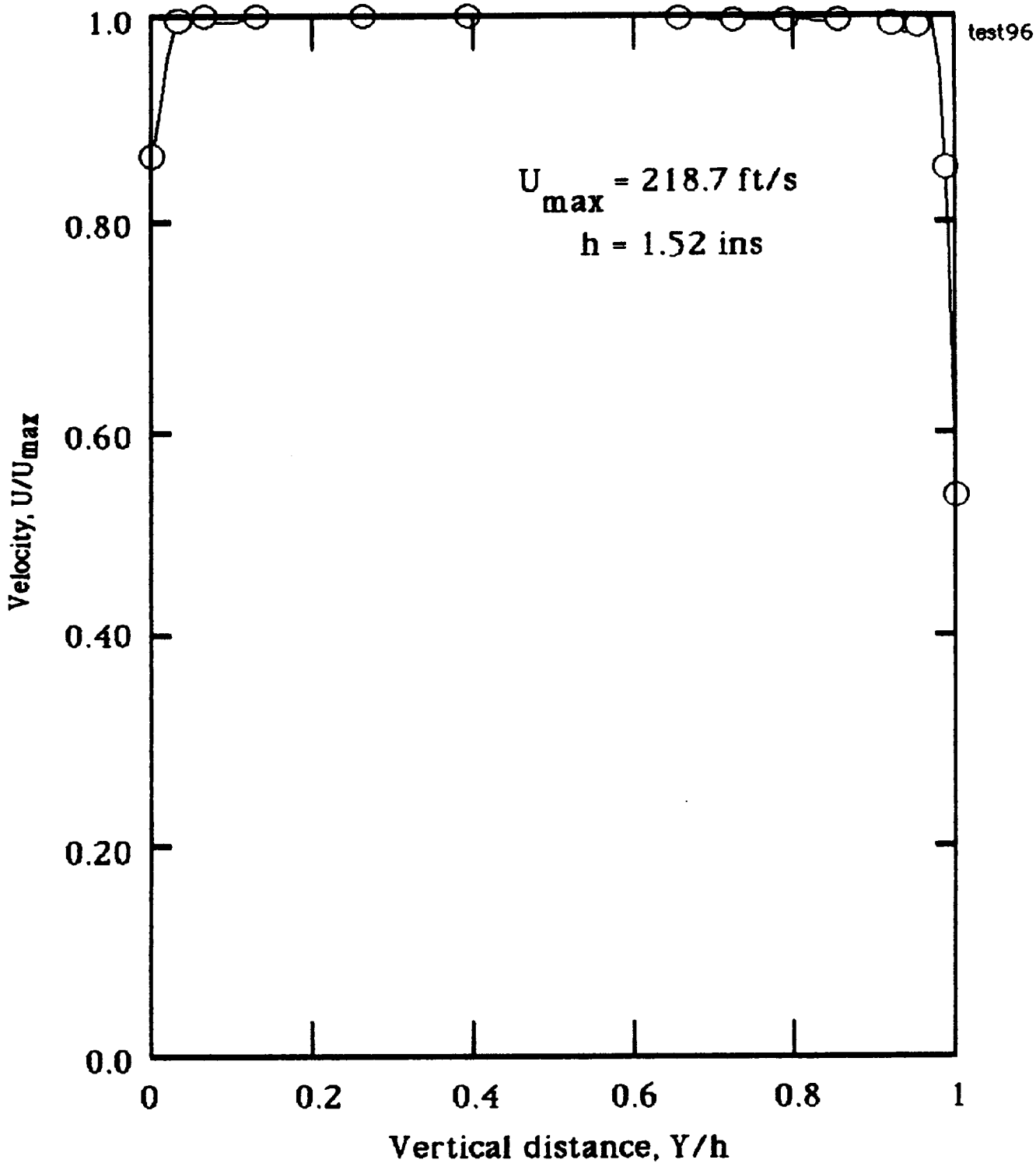

Figure 13. Vertical variation of flow velocity across the centerline of the contraction exit plane with the air vent closed.

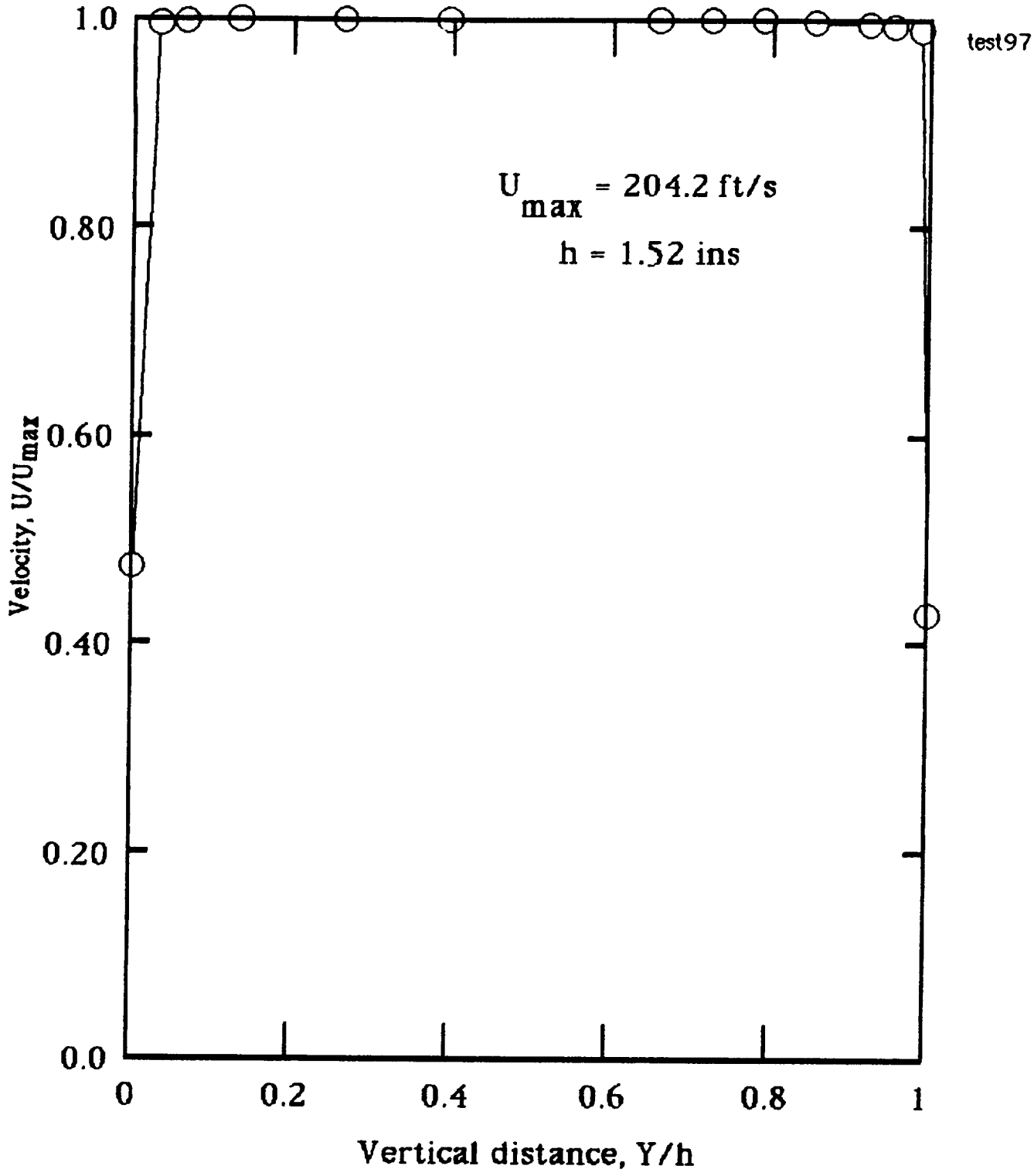

Figure 14. Vertical variation of flow velocity across the centerline of the contraction exit plane with the air vent open.

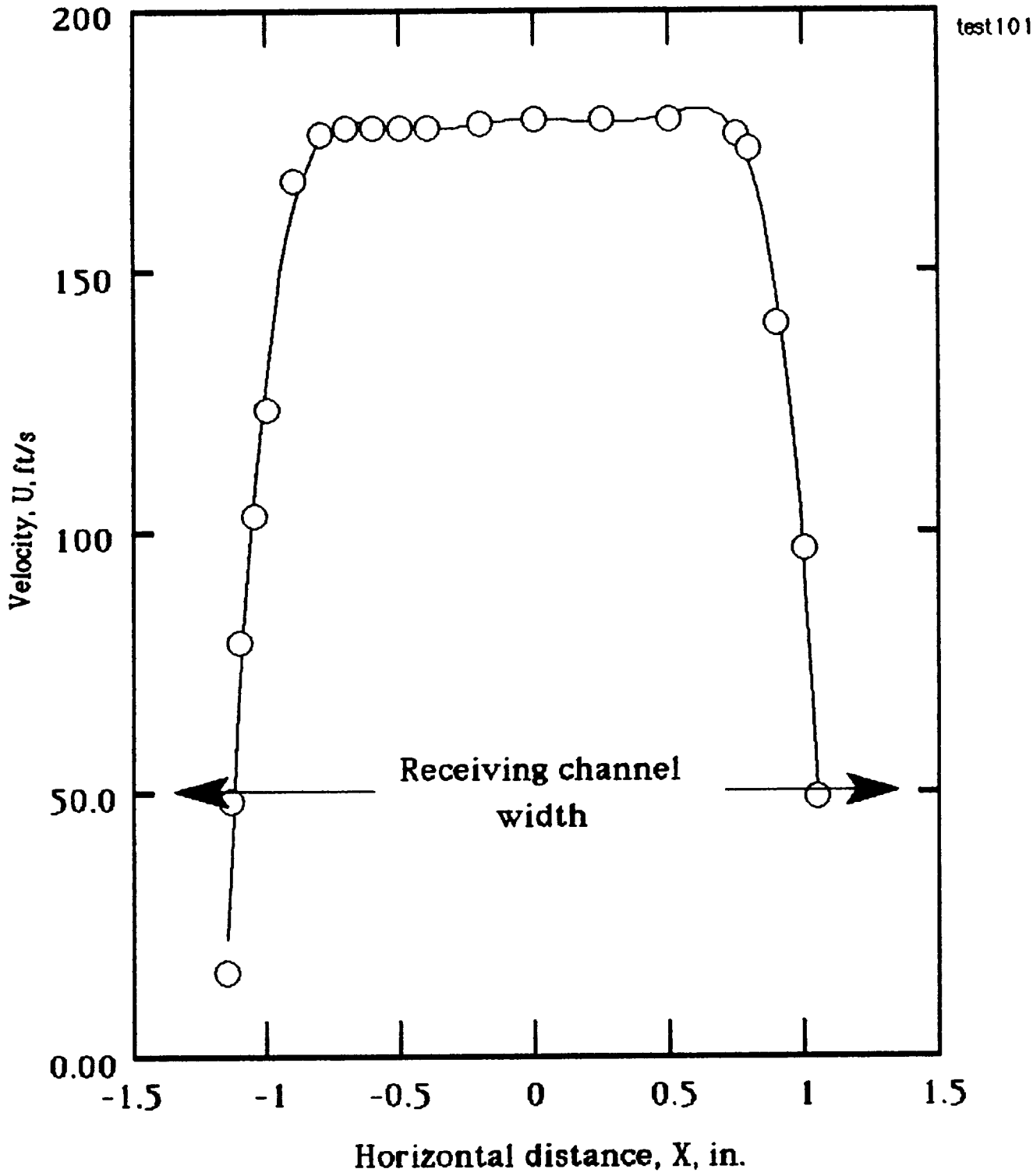

Figure 15. Horizontal variation of flow velocity across the centerline of the diffuser intake, with the air vent closed.

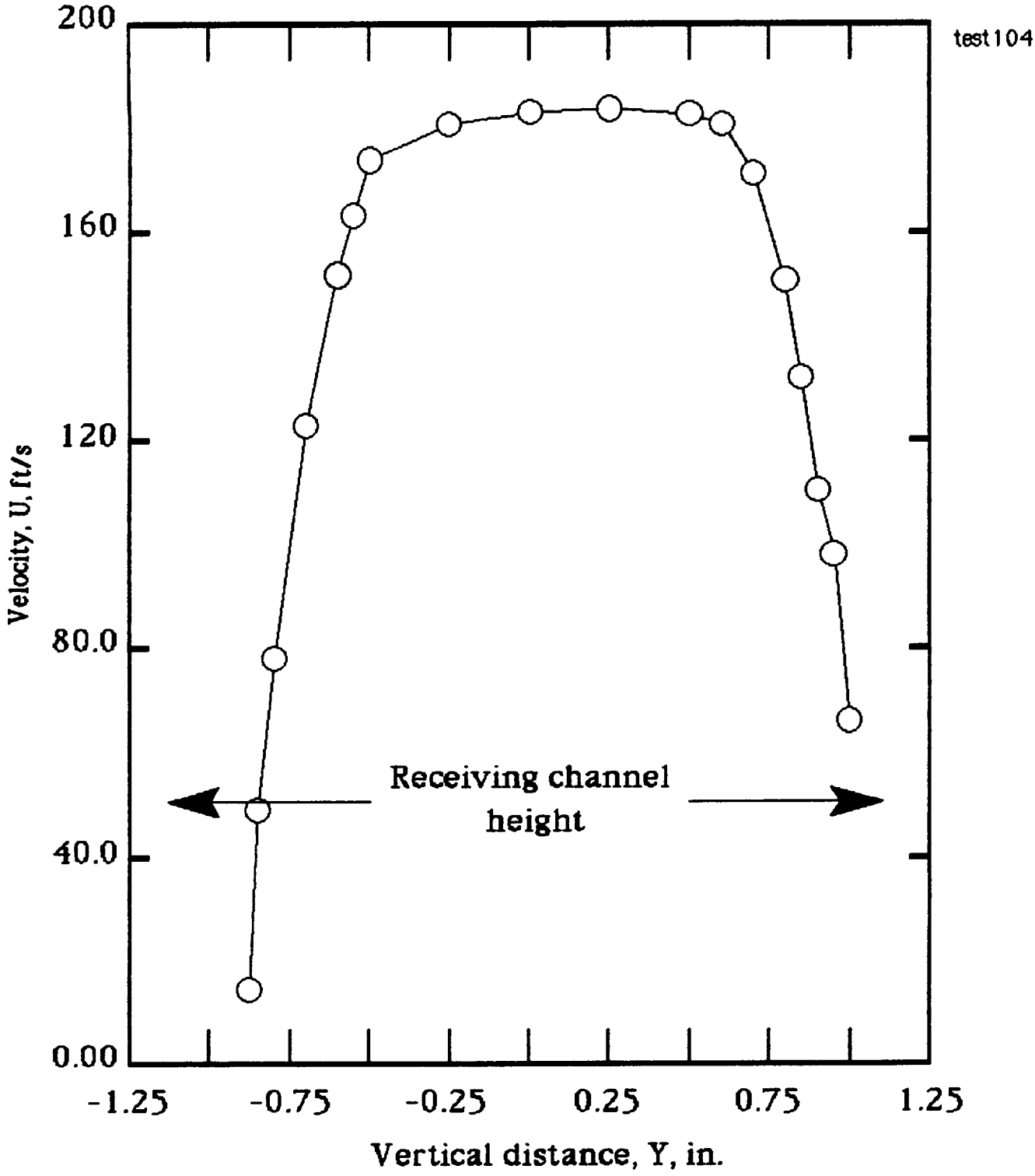

Figure 16. Vertical variation of flow velocity across the centerline of the diffuser intake, with the air vent closed.

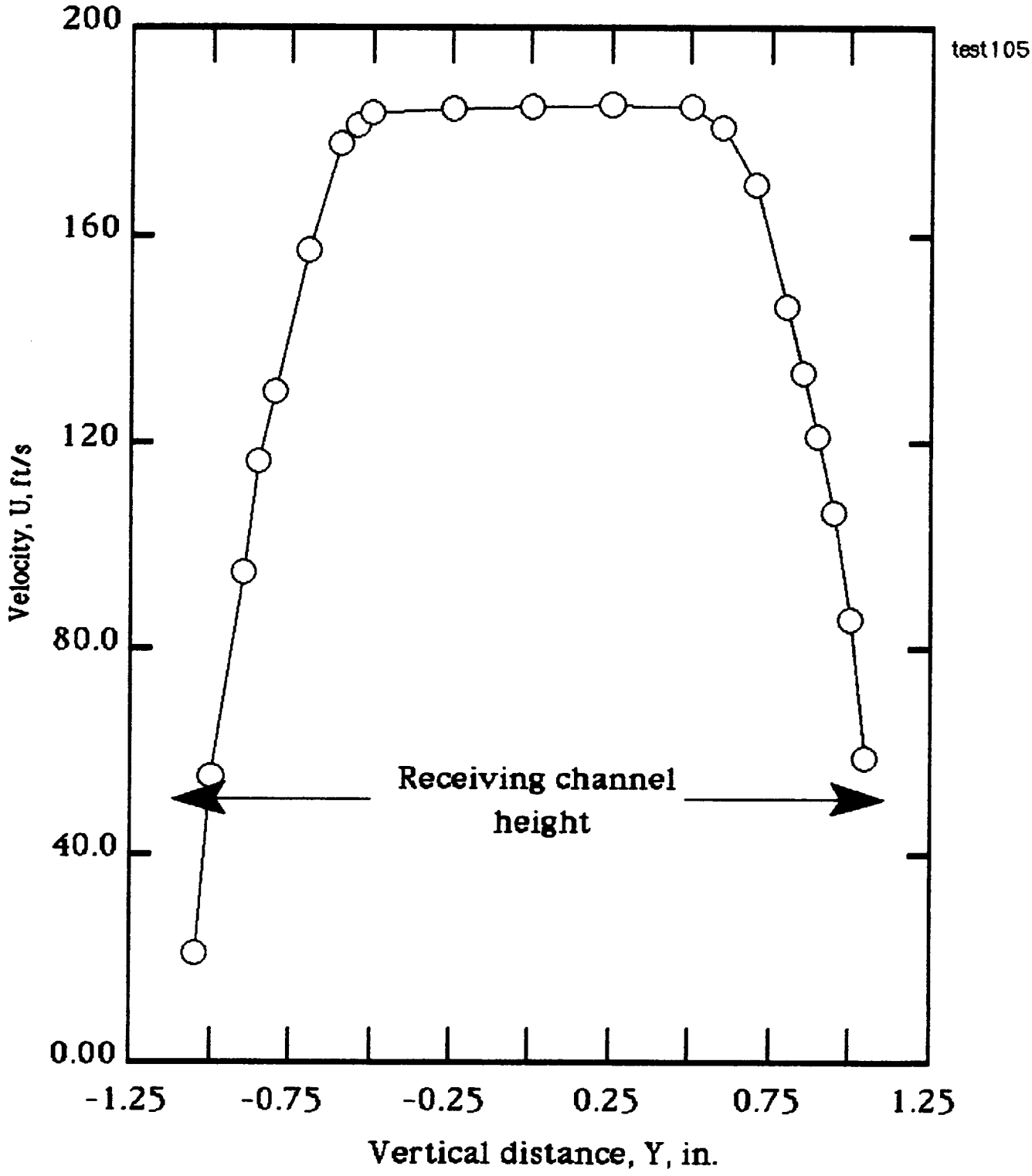

Figure 17. Vertical variation of flow velocity across the centerline of the diffuser intake, with the air vent open.

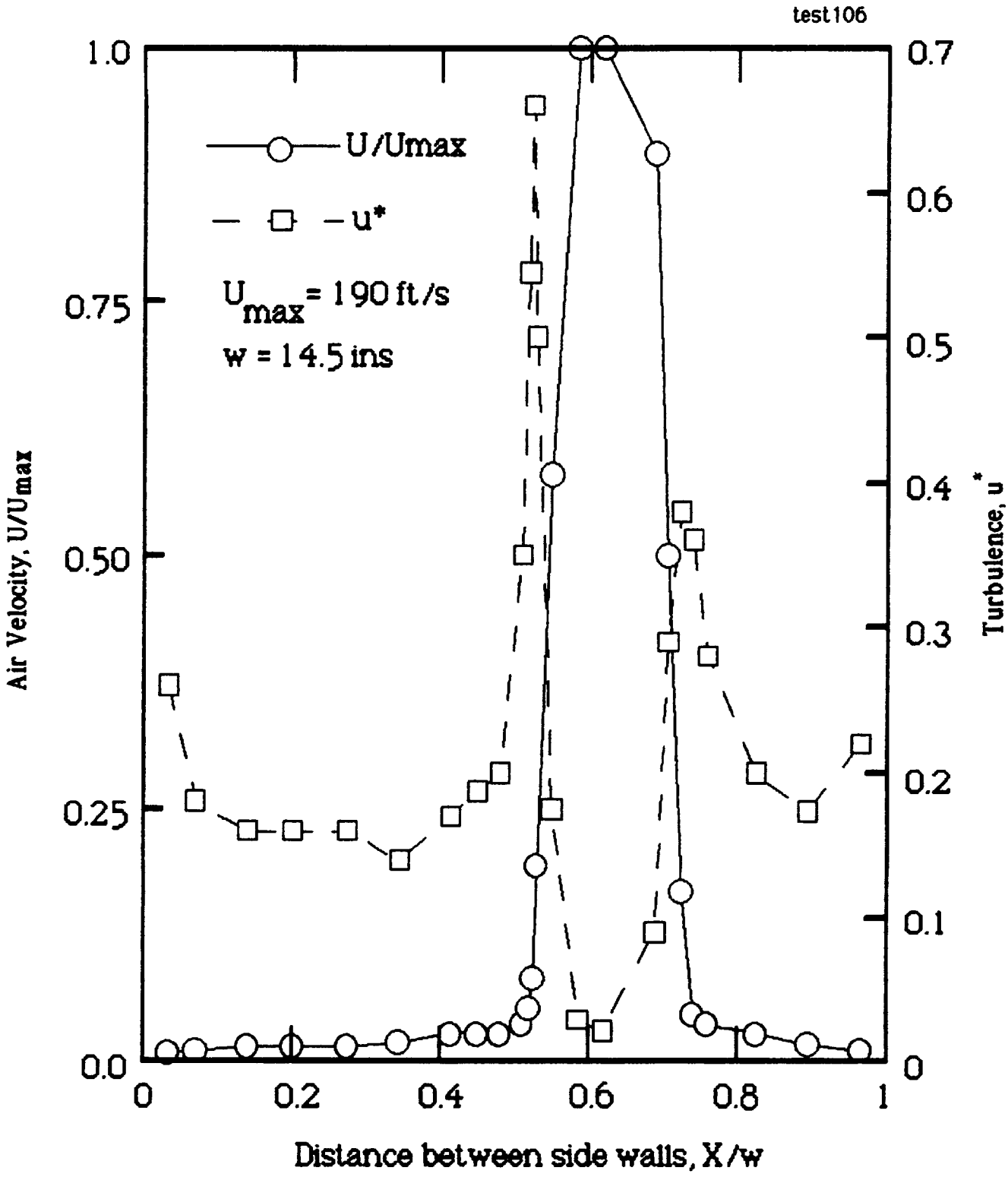

Figure 18. Horizontal variation of velocity and turbulence at the diffuser entrance, with the air vent open.

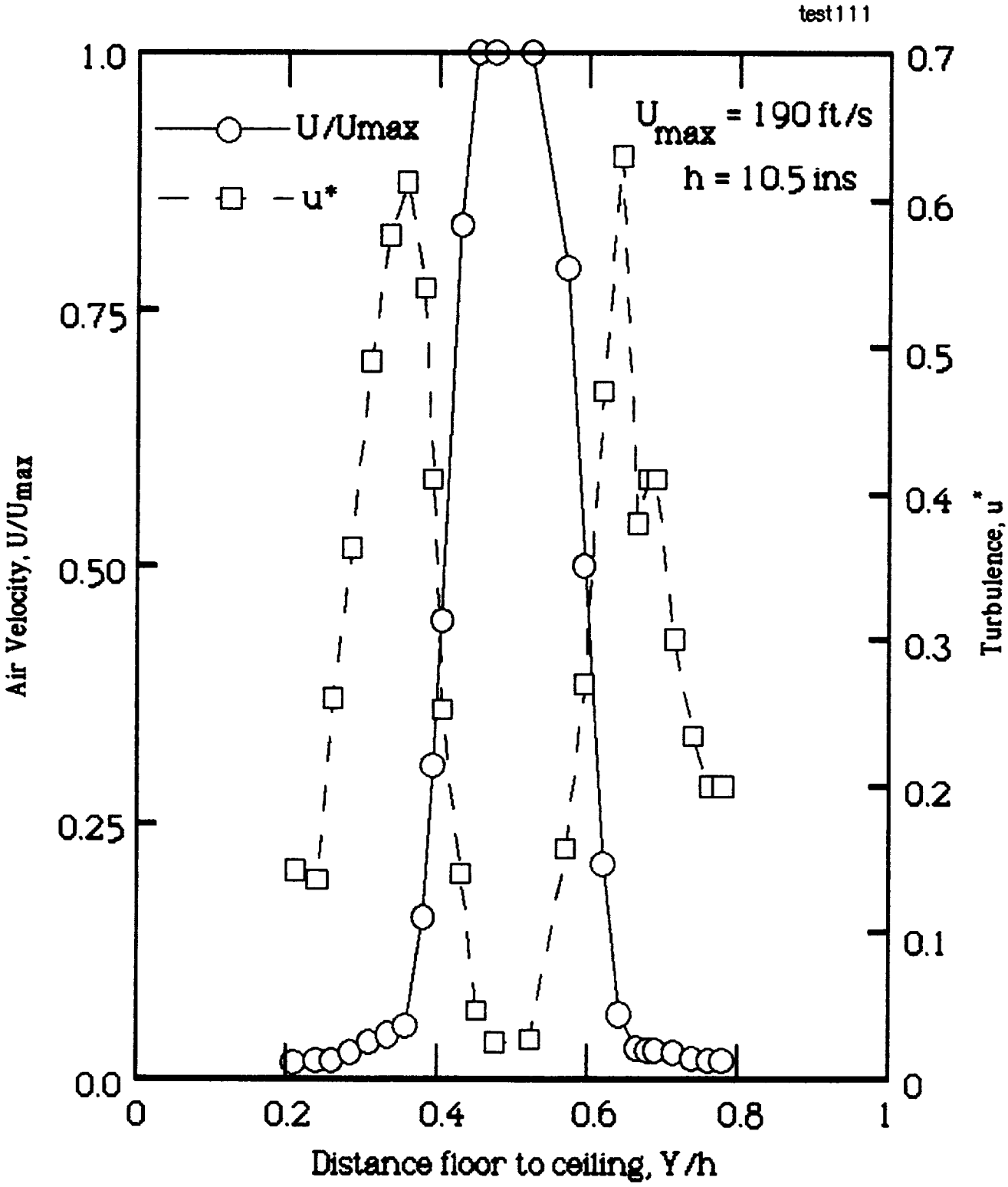

Figure 19. Vertical variation of velocity and turbulence at the diffuser entrance, with the air vent closed.

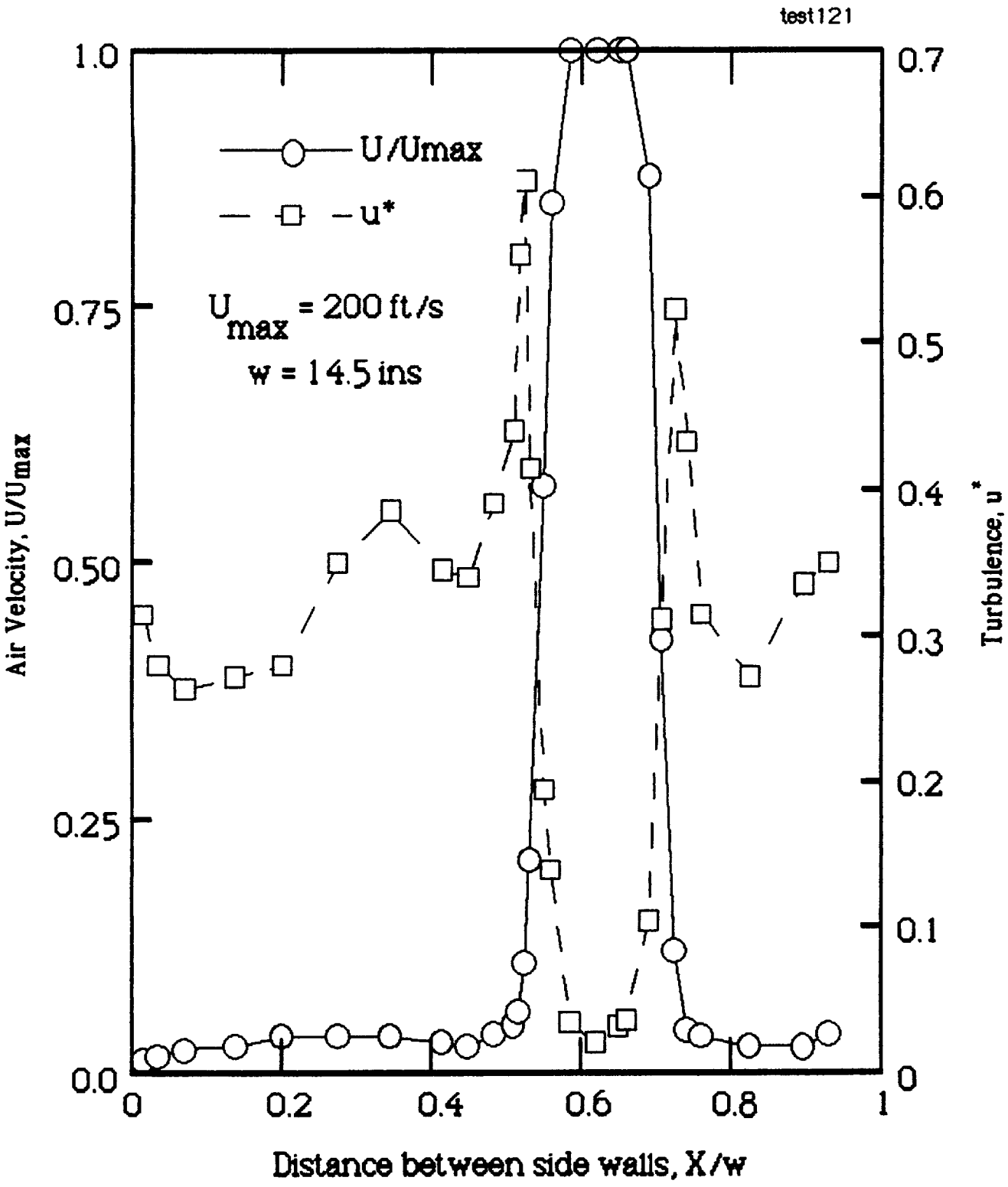

Figure 20. Horizontal variation of velocity and turbulence at the diffuser entrance, with the air vent closed.

REPORT DOCUMENTATION PAGE

Form Approved
OMB No. 0704-0188

1. AGENCY USE ONLY (*Leave blank*)	2. REPORT DATE	3. REPORT TYPE AND DATES COVERED
	April 1995	Contractor Report

4. TITLE AND SUBTITLE

Results of Tests Performed on the Acoustic Quiet Flow Facility Three-Dimensional Model Tunnel
Progress Report on the D.S.M.A. Design

5. FUNDING NUMBERS

C NAS1-19000
WU 538-03-12-01

6. AUTHOR(S)

P. S. Barna*

7. PERFORMING ORGANIZATION NAME(S) AND ADDRESS(ES)

Lockheed Engineering & Sciences Company
Hampton, VA 23666

8. PERFORMING ORGANIZATION REPORT NUMBER

9. SPONSORING / MONITORING AGENCY NAME(S) AND ADDRESS(ES)

National Aeronautics and Space Administration
Langley Research Center
Hampton, VA 23681–0001

10. SPONSORING / MONITORING AGENCY REPORT NUMBER

NASA CR-198311

11. SUPPLEMENTARY NOTES

Langley Technical Monitor: J. W. Posey

12a. DISTRIBUTION / AVAILABILITY STATEMENT

Unclassified-Unlimited
Subject Category: 71

12b. DISTRIBUTION CODE

13. ABSTRACT (*Maximum 200 words*)

The test results briefly described in this report were obtained on the three-dimensional 1:48 scale tunnel modeled on the design proposed by Messrs. D.S.M.A. Corporation. More particularly, while the test chamber dimensions were indeed scaled down in the ration of 1:48, including the contraction and the collector as well, the duct system itself leading to and from the chamber was adapted to suit laboratory conditions and space limitations.

Earlier tests with the two-dimensional model showed that blowing mode was preferred as against the suction mode, hence all tests were performed with blowing only. At the exit of the contraction the maximum airspeed attained with the 1 HP blower unit was about 200 ft/sec. This airspeed may be increased in future if desired.

The test results show that pressure recovery in the diffuser was about 34 percent due to the large blockage at its entrance. Velocity traverses taken across the diffuser entrance explain the reason for this blockage. Recirculation, studied with both, hot-wire anemometry and flow-visualization techniques, was largely affected by the design of the test chamber itself and the amount of vent-air admitted to the chamber. Vent-air helped to decrease the level of turbulence.

14. SUBJECT TERMS

wind tunnel, open jet, jet entrainment, scale model flow facility, nozzle-diffuser, jet collector

15. NUMBER OF PAGES

32

16. PRICE CODE

A03

17. SECURITY CLASSIFICATION OF REPORT	18. SECURITY CLASSIFICATION OF THIS PAGE	19. SECURITY CLASSIFICATION OF ABSTRACT	20. LIMITATION OF ABSTRACT
Unclassified	Unclassified	Unclassified	